Advanced Remote Sensing

http://publish.mersin.edu.tr/index.php/arsej

e-ISSN 2979-9104

Integration of Sentinel-1 and Landsat-8 images for crop detection: The case study of Manisa, Turkey

Muslum Altun [*1], **Mustafa Turker** [1]

[1]*Hacettepe University, Department of Geomatics Engineering, Türkiye, altunmuslum06@gmail.com, mturker@hacettepe.edu.tr*

Cite this study: Altun, M., & Turker, M. (Year). Integration of Sentinel-1 and Landsat-8 images for crop detection: The case study of Manisa, Turkey. Advanced Remote Sensing, 2(1), 23-33

Keywords
SAR and Optical Image Classification
Crop Detection
Random Forest (RF)
Image Fusion

Research Article
Received: 24.05.2022
Revised: 20.06.2022
Accepted: 25.06.2022
Published: 30.06.2022

Abstract

In this study, the accuracy performance of crop detection through classification was investigated in the integration of Sentinel-1 Vertical-Vertical (VV) and Vertical-Horizontal (VH) polarized Synthetic Aperture Radar (SAR) and Landsat-8 satellite images belonging to a single date. A study area was selected from a region with dense agricultural lands within the boundaries of Manisa, Turkey. Wheat, Tomato, Corn, Corn_2, Cotton, Grapes, Clover and Olive Trees were determined as the crop types. Feature level integration was used to generate image stack and random forest (RF) machine learning algorithm was used for image classification. Classification was carried out using only Sentinel-1 SAR data, only Landsat-8 optical data and the merged data set of Sentinel-1 VV+VH and Landsat 8. Image stacking of Sentinel-1 VV+VH and Landsat 8 increased the classification accuracy. The highest overall accuracy (81.46%) was achieved through classification based on the stacked dataset of the Sentinel-1 VV+VH bands and the Landsat-8 optical bands. The study has shown that the stacked dataset of Sentinel-1 VV+VH and Landsat-8 belonging to a single date has great potential in extracting summer crop types.

1. Introduction

One of the most common uses of earth observation satellites is the detection of agricultural products [1-2]. The information provided by thematic maps obtained from satellite images is very useful for the effective management, monitoring, decision making and computing the statistics of the crops produced in agricultural areas [3-4].

Remote sensing applications in agriculture are performed using the optical and Synthetic Aperture Radar (SAR) images [5-6]. Crop detection is among the most common uses of satellite images in agricultural areas. Although significant progress has been made in classification and crop detection using the optical satellite images, it is not always possible to find images of the desired dates and therefore to extract the necessary information due to constraints, such as cloud cover and temporal resolution. Unlike optical satellites, SAR satellites employ active sensors that provide their own energy for image acquisition. Among the important advantages of SAR satellites are that they are not affected by the weather conditions and have the ability to receive images day and night. For this reason, the use of radar images in the detection of crop types in agricultural areas is becoming more common day by day.

Due to various limiting effects, the combined use of optical and SAR satellite data sets has become inevitable. Their combined use, which is prominent in distinguishing different crop types, increases the interest in agricultural studies [7]. Many studies have been conducted to classify agricultural areas and detect agricultural crops from satellites with different sensors [8-9].

Remote sensing data acquisition is very expensive in terms of time and cost analysis. In this respect, the availability of Sentinel and Landsat satellite images free of charge is very important as they eliminate this difficulty. In addition, Landsat-8 satellite stands out with its wide use in many different areas in terms of its rich band number, providing images with different spatial resolutions to users, and low temporal resolution feature of Sentinel-1 satellite enables images to be used in a short time. With these features, agriculture has become one of the most common usage areas of Sentinel-1 and Landsat-8 images. The use of Sentinel-1 images is of particular importance for crop pattern detection in regions where it is difficult to obtain clear optical images or where a sufficient number of images cannot be obtained [8-11].

Based on the literature search on the related subject, [12] fused the Sentinel-1 SAR image dated April 15, 2018 and April 22, 2018 and Landsat-8 OLI bands dated April 26, 2018 using Decision Level Fusion (DLF) technique and performed classification using the Support Vector Machines (SVM) algorithm. In their study, SAR VV+VH polarized bands were used. The effect of the speckle filter on the results was also measured in the study. In the classification performed using the bands fused with DLF technique without applying a speckle filter, 96.02% overall accuracy and 0.9515 kappa coefficient were obtained. It was observed that the speckle filter reduces the classification accuracy and texture properties produced from the VH polarized band outperformed those produced from VV polarized band.

In the study of [13], resolution merge and The Local Mean Variance Matching (LMVM) data fusion techniques were compared using the Sentinel-1 SAR image dated February 25, 2015 and the Landsat-8 OLI image dated March 18, 2015. As the images, the VV and VH polarized bands of Sentinel-1A were used. Four datasets, Sentinel-1A SAR, Landsat-8 OLI, Resolution merge (Sentinel-1 + Landsat 8) and LMVM (Sentinel-1 + Landsat 8), were used in classification performed using the Maximum Likelihood (ML) algorithm. Based on the results obtained, 58.50% overall accuracy and 0.48 kappa coefficient were calculated when using only Sentinel-1A SAR data, 67.16% overall accuracy and 0.59 kappa coefficient accuracy values were calculated when using only Landsat 8 OLI data, and 79.75% overall accuracy and 0.75 kappa coefficient values were calculated when using the fused data set of Sentinel-1 and Landsat-8 based on resolution merge. In the classification performed using Sentinel 1 + Landsat 8 data fused with the LMVM technique, 59.84% overall accuracy and 0.52 kappa coefficient values were calculated.

In the study of [14], 2.75 m resolution TerraSAR-X and 30 m resolution Landsat ETM+ images were fused using high pass filtering (HPF), Principal Component Analysis with band substitution (PCA) and Principal Component with Wavelet Transform (WPCA) image fusion techniques. Then, the fused images were classified by the decision tree algorithm. Overall accuracy of 74.99%, 83.12% and 85.38%, respectively, and kappa coefficient values of 0.7220, 0.8100, and 0.8369 were obtained from the fused images based on HPF, PCA and WPCA techniques. It was stated that WPCA is the most suitable one among the fusion techniques used.

In the study of [15], Landsat 8 and Sentinel-1 SAR image were fused with the RGB Transformation and Brovey Transformation methods, and their morphology was extracted to sharpen the appearance of lava flow deposits in volcanoes. Sentinel-1 VV polarized band was used in the study. The results were visually analyzed by comparing with the figures. According to the results, the images and techniques used showed that the volcanoes can be observed continuously in all weather conditions.

In the study of [16], Sentinel-1 SAR and Landsat 8 OLI images were fused with the Wavelet, Ehlers, Principal Component Analysis (PCA) and Gram-Schmidt (GS) methods to distinguish summer crop areas, garden areas and orchard areas in the Fergana Valley, Uzbekistan. Images fused with each method were classified using the SVM, Nearest Neighborhood (NN), Random Forest (RF) and Naive Bayesian (NB) algorithms. Classification using RF algorithm on the data set obtained through fusing with the Ehlers method gave the highest overall accuracy of 85.9%.

In the study of [17], paddy crops were detected using the classification of the Normalized Difference Vegetation Index (NDVI) bands derived from Sentinel-1 SAR and Landsat 7 Enhance Thematic Mapper-Plus (ETM+) and Landsat 8 OLI images in Heilongjiang, China. In their study, SAR VV and VH bands and NDVI bands were used together by means of fusing them. The classification was performed using the SVM and RF algorithms. Classification of SAR data in the VH polarized state based on RF algorithm provided the best results with an overall accuracy of 0.94 and a kappa coefficient of 0.93.

In the study of [18], classification was carried out using the RF algorithm on the fused 12 Sentinel-1A, -1B SAR and Landsat-8 data collected at different times in 2015 and 2016 in Sub-Saharan Africa, inside and outside the residential areas. The VV and VH polarization bands of the SAR data were used. It was stated that the VV polarization band performed better than VH. Texture features were created and analyzed with Gray Level Co Occurrence Matrix (GLCM) in different window sizes. Optical and SAR data were combined using PCA image fusion technique. Optical data only, SAR data only, and the fused SAR and optical data were classified using pixel-based RF algorithm. It was stated that classification performed on the fused images provided quite high performance compared to the others.

In the study of [19], image classification was performed to find the best land weave in the Pearl River Delta (PRD) region of China. In their study, the fusion was carried out between the 30 m resolution Landsat ETM+ and 75 m resolution ENVISAT ASAR (WSM) image; 10 m resolution SPOT-5 and 12.5 m resolution ENVISAT ASAR (IMP) image; 10 m resolution SPOT-5 and 3 m resolution TerraSAR-X image. Image fusion was performed using the Pixel

level, Feature Level A, Feature Level B and Decision Level fusing techniques. Classification of the fused images was carried out using the ML, Artificial Neural Network (ANN), SVM and RF algorithms. The fused image obtained with the Feature Level B technique and the classification made by ML, ANN, SVM and RF algorithms provided better performance than other fusion methods (0.92 overall accuracy and 0.96 kappa coefficient).

In this study, we aim to classify the feature level image stacked Sentinel-1 Synthetic Aperture Radar (SAR) (Vertical Vertical-VV and Vertical Horizontal-VH bands) and Landsat-8 data belonging to a single date (07.06.2017) using a machine learning algorithm. We investigate the effect of the stacked dataset of single date Sentinel-1 and Landsat 8 on the performance of crop classification. The agricultural area located between Salihli and Ahmetli districts of the city of Manisa, Turkey was chosen as the study area. As the images, 10 m resolution Sentinel-1 VV and VH polarized bands and 30 m resolution Landsat-8 Coastal Aerosol, Blue, Green, Red, Near Infrared, Short-Wave Infrared 1 and Short-Wave Infrared 2 bands were used. Image integration was performed. RF machine learning algorithm was chosen as the classifier. The detected crops are wheat, tomatoes, corn, corn2, cotton, grapes, clover and olive trees that are the most widely planted crop types in the region. The contribution of the combined use of the Sentinel-1 and Landsat 8 dataset on the accuracy of crop classification is shown by the computed accuracy values.

2. Study Area and Data

An agricultural area with the size of 520 km^2 located within the borders of Ahmetli and Salihli Districts of the city of Manisa, Turkey was selected (Figure 1). The approximate coordinates of the study area are; 573369.16 m, 4275559.88 m (North West); 573369.16 m, 4257782.09 m (South West); 603175.50 m, 4275559.88 m (North East); 603175.50 m, 4257782.09 m (South East) with the projection information of WGS 84, UTM-Zone 35 N, and Central meridian 27.

In the study area, most of the parcels are cultivated with the summer crops as well as fallow areas and non-agricultural areas that are not cultivated. The main crops grown in the region are include wheat, tomatoes, corn, cotton, grapes, clover, and olive trees.

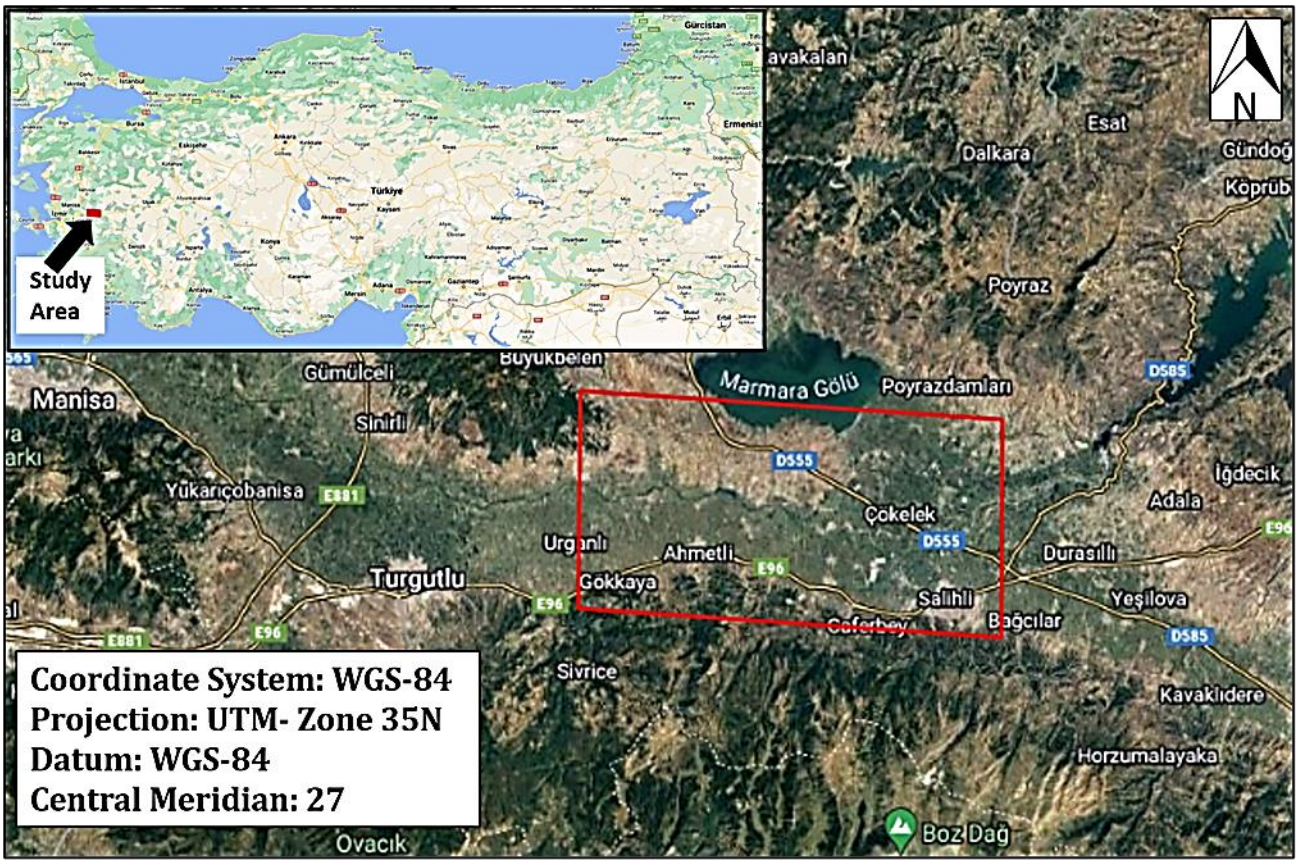

Figure 1. Study area

The Sentinel-1 SAR and Landsat-8 images covering the study area were visually examined and both images acquired on the same date (07.06.2017) were selected as image data. VV and VH polarized C bands of Sentinel-1 SAR and the Coastal Aerosol, Blue, Green, Red, Near Infrared, Shortwave Infrared 1 and Shortwave Infrared bands of Landsat-8 were downloaded from the relevant sites [20-21]. The downloaded data files also contain metadata information, such as projection, geometric and radiometric correction files, etc. The spatial resolutions of the VV

and VH polarized SAR C bands and the Landsat-8 Coastal Aerosol, Blue, Green, Red, Near Infrared, Short-Wave Infrared 1 and Short-Wave Infrared 2 optical bands are given in Table 1.

Table 1. Bands and spatial resolutions of Sentinel-1 and Landsat-8 images

Satellite	Band	Spatial Resolution (m)
Sentinel-1	C band – VV polarization	10
	C band – VH polarization	10
Landsat-8	Band 1 – Coastal Aerosol	30
	Band 2 – Blue	30
	Band 3 – Green	30
	Band 4 - Red	30
	Band 5 - NIR	30
	Band 6 – SWIR 1	30
	Band 7 – SWIR 2	30

Farmer Registration System (FRS) is an agricultural database which contains information about the farmers to ensure that agricultural supports can be monitored, audited, reported and questioned [22]. In this study, we used the existing FRS data as the ground truth reference data. While the spatial information of the FRS data includes the location information, the attribute information consists of land registry information such as, province name, district name, parcel ID, parcel area, cultivated area, cultivated crop types, etc.

3. Methodology

The flowchart summarizing the steps of the method is shown in Figure 2. The method consists of four main steps: data preprocessing, image integration, classification and accuracy analysis. First, the necessary preprocessing steps were applied to Sentinel-1 SAR and Landsat-8 optical images. Then, the necessary arrangements were made on the FRS data so that it can be used as ground reference data. In the second step, feature level integration between Sentinel 1 SAR and Landsat-8 optical images was performed through image stacking. Parcel-based classification of the stacked image dataset was then carried out using the RF machine learning algorithm. As the final step, accuracy assessment of the obtained results was performed.

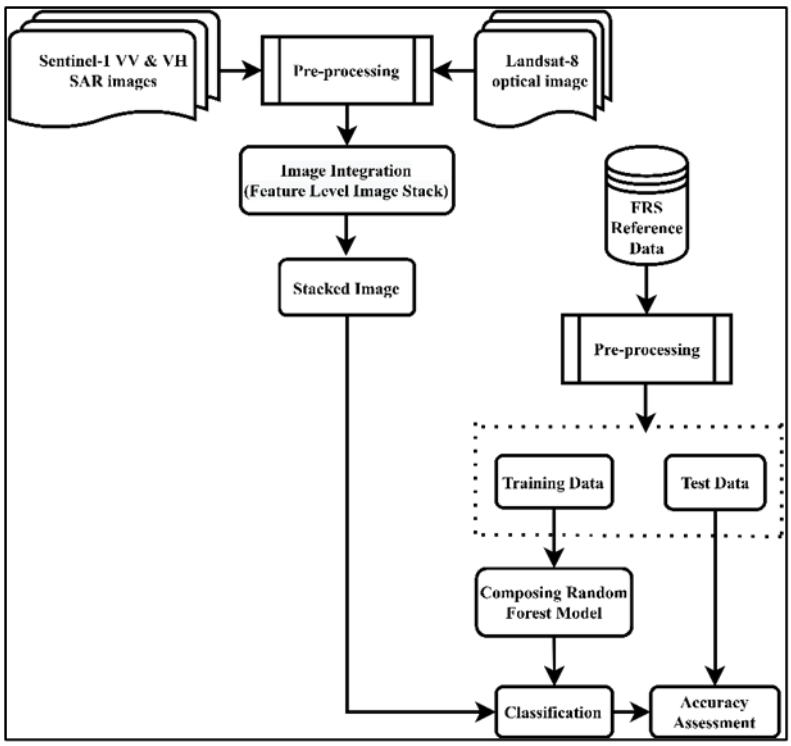

Figure 2. The flowchart of the methodology

3.1. Data pre-processing

Preprocessing operations were applied to Sentinel-1 VV and VH polarized data using the Sentinel Application Platform (SNAP) software [23]. Apply orbit file, radiometric calibration, speckle filtering (Lee Filter 5x5), topographic correction and back reflection db conversion preprocessing steps were performed. With the preprocessing applied to orbit file, the correct satellite position and velocity information was obtained by bringing up-to-date corrections to the satellite orbital state vectors of the SAR data. With radiometric calibration, the pixel values were converted to radiometrically calibrated SAR back reflection values. The speckle noise was reduced by applying a 5×5 Lee filter [24-25]. Distortions caused by topography were corrected with terrain correction and therefore the image was geometrically brought closer to the real earth. In the back-reflection dB conversion step, the back-reflection coefficients without any unit value were converted into dB using the logarithmic transformation given in Equation 1 [25].

$$\beta_{db}^{0} = 10 * \log_{10}(\beta^{0}) \quad (1)$$

Preprocessing for the Landsat-8 optical satellite image consists of producing a layer stack of the bands to be used in classification [26]. The VV, VH and VV+VH polarized Sentinel-1 SAR data and Landsat-8 optical image obtained after the preprocessing steps are illustrated in Figure 3.

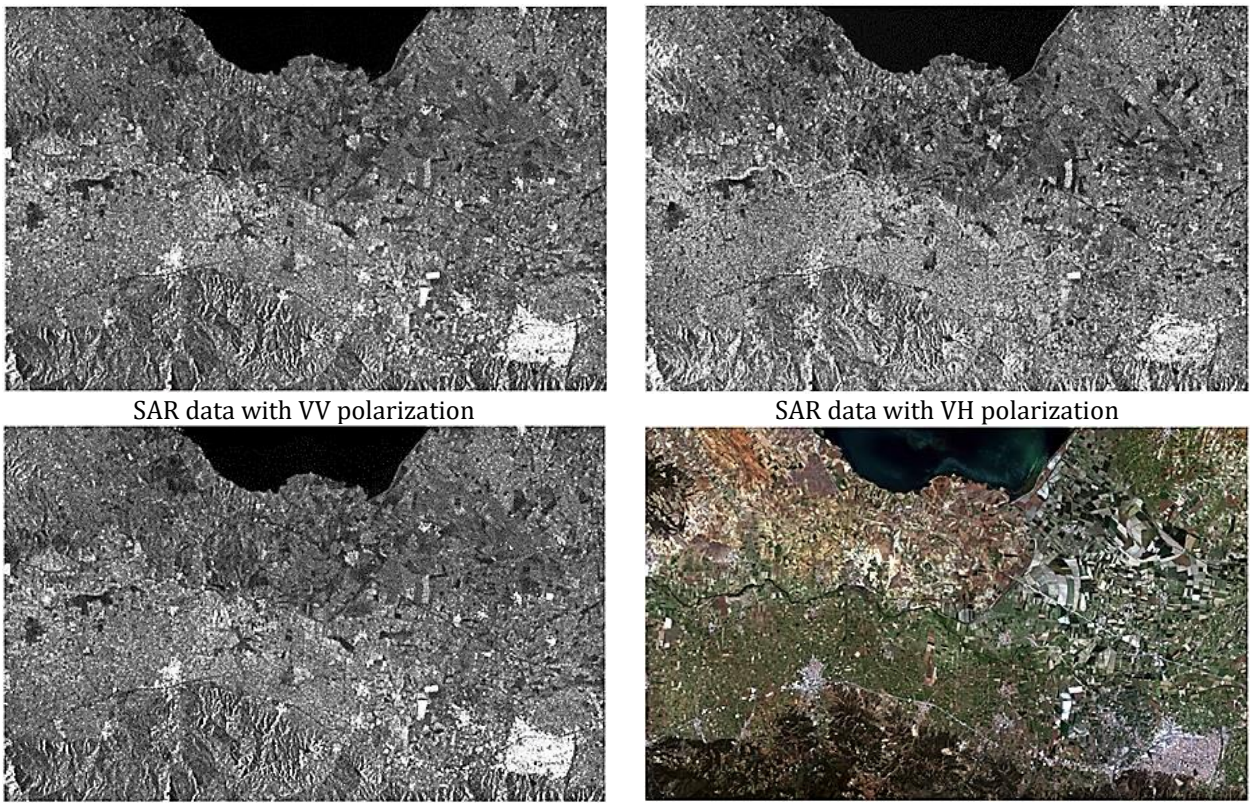

SAR data with VV polarization | SAR data with VH polarization

SAR data with VV and VH polarization | Landsat-8 (True Color - Blue, Green, Red)

Figure 3. Landsat-8 and Sentinel-1 SAR images after pre-processing

In addition to images, the necessary preprocessing operations were also performed on the reference data (FRS data). Parcels smaller than 1000 m^2 were eliminated as most of these parcels did not contain a crop. The crops grown in the parcels and the spatial data of the parcels (polygon) were associated.

3.2. Integration of Sentinel-1 SAR and Landsat-8 optic images

In this study, we used feature level image integration to combine Sentinel-1 SAR (VV and VH bands) and Landsat-8 image (multi-spectral bands) data sets [27]. Our purpose for image integration was to obtain an integrated multi-band dataset from the combination of Sentinel-1 SAR image and Landsat 8 optical image. The higher spatial resolution Sentinel-1 SAR VV and VH bands were chosen as the first input data, while the lower spatial resolution multi-band (7-band) optical Landsat 8 image was chosen as the second input data. Image integration was performed using the "Composite Bands" tool of the ArcGIS software. With this tool, one can also create a raster dataset containing a subset of the original bands. This is useful if you need to create a new raster

dataset with a specific band combination and order [26]. The output raster dataset (in this study feature level integrated image) takes the cell size (spatial resolution) from the first raster band (in this study 10 m resolution Sentinel-1 SAR-VV and VH bands) in the order of inputs. Therefore, in this case, the spatial resolution of the feature level integrated data set has become 10 m.

3.3. Image classification

Image classification was carried out in MATLAB R2019b using the RF machine learning algorithm [29]. RF is one of the ensemble algorithms that uses the decision tree as the base class [30]. Before starting the tree development process, two parameters must be defined by the user to start the RF algorithm. These parameters are the number of variables (mtry) used at each node and the number of trees to be developed (ntree). The RF algorithm combines classifications made by many individual decision trees [28]. When the defined number of trees (ntree) is produced, the class of the candidate pixel is determined based on the estimation results obtained from the ntree tree [30]. In this study, the ntree value was taken as 100, and the mtry value was calculated as $\sqrt{\text{number of bands}}$ following [31]. In the present case, we used a parcel-based classification approach. In parcel-based classification, pixel groups are created according to certain characteristics of the pixels such as shape, color, texture, size, relationship and pattern, and operations are performed on these pixel groups [32-33]. In this study, we used the FRS parcel boundaries to define homogeneous pixel groups. For each parcel, the frequencies of the classified pixels were calculated and the label of the highest frequency class was assigned to all pixels falling within the parcel. Of the 1024 reference parcels, 512 were used as training and 512 were used to test the classification accuracy.

Wheat, Tomato, Corn, Corn_2, Cotton, Grapes, Clover and Olive Trees were defined as the crop types (classes) to be classified. As a result of the analysis of the images and FRS data we noticed that there were two types of corn. Therefore, corn was divided into two different classes (Corn and Corn_2). The number of parcels and pixels used for training and validation are given in Table 2. Image classification was performed using five different image data sets and the results were compared. In particular, the effect of the stacked dataset of Sentinel-1 SAR and Landsat-8 on classification accuracy was evaluated. The image data sets used for classification are as follows: i) Sentinel-1 VV band only, ii) Sentinel-1 VH band only, iii) Sentinel-1 VV and VH bands together, iv) Landsat-8 data only, and v) Stacked dataset of Sentinel-1 VV+VH bands and Landsat-8 data.

Table 2. The number of parcels and pixels used for training and validation

Agricultural Crop	Training Data (Parcel / Pixel)		Test Data (Parcel / Pixel)	
Wheat	94	37852	94	11473
Tomato	26	12880	26	4399
Corn	78	26636	78	10480
Corn_2	25	7661	25	3628
Cotton	28	15090	28	7020
Grapes	202	33996	202	14398
Clover	8	6027	8	563
Olive Trees	51	27482	51	11670
Total	512	167624	512	63631
Overall total	1024/231255			

4. Results and Discussion

For the accuracy assessment of the classified images, we used a standard error matrix. Since the classification was conducted based on parcel basis, we performed accuracy assessment on parcel-basis, therefore. In determining the number of test parcels, the study of [30] was taken into account. From the error matrix [34], we computed the overall accuracy and Kappa coefficient values. In addition, producer's accuracy (PA) value and user's accuracy (UA) value were also calculated for each class. The calculated accuracy values are given in Table 3. Figure 4 shows the graphical comparison of overall accuracy and Kappa coefficient values of the classified outputs. The classified images using different data sets are shown in Figure 5 (a-e).

Table 3. Classification accuracy values computed based on different data sets. (PA: Producer Accuracy, UA: User Accuracy, VV: Vertical-Vertical Polarization, VH: Vertical-Horizontal Polarization)

Crop Type	Sentinel-1 VV		Sentinel-1 VH		Sentinel-1 VV+VH		Landsat-8		Stacked Sentinel-1 VV+ VH and Landsat-8	
	PA (%)	UA (%)	PA (%)	UA (%)	PA (%)	UA (%)	PA (%)	UA (%)	PA (%)	UA (%)
Wheat	48,00	48,42	50,62	51,06	58,62	59,13	60,10	64,55	62,98	68,86
Tomato	30,57	32,11	32,23	33,86	37,33	39,21	76,16	78,33	73,06	82,08
Corn	36,76	42,59	38,76	44,91	44,89	52,01	66,28	72,73	78,13	75,54
Corn_2	22,71	25,64	23,94	27,03	27,73	31,31	81,16	80,58	89,79	88,58
Cotton	36,04	41,87	38,00	44,15	44,01	51,13	80,72	77,14	81,91	80,34
Grapes	42,99	47,41	45,33	49,99	52,50	57,90	74,19	74,87	89,27	88,31
Clover	41,51	39,79	43,78	41,96	50,70	48,60	76,12	77,76	88,60	87,10
Olive Trees	25,52	29,65	26,91	31,27	31,17	36,21	71,63	73,90	86,65	91,46
Overall Accuracy	34,12		35,98		41,67		71,18		81,46	
Kappa Coefficient	30,22		31,87		36,92		63,06		76,24	

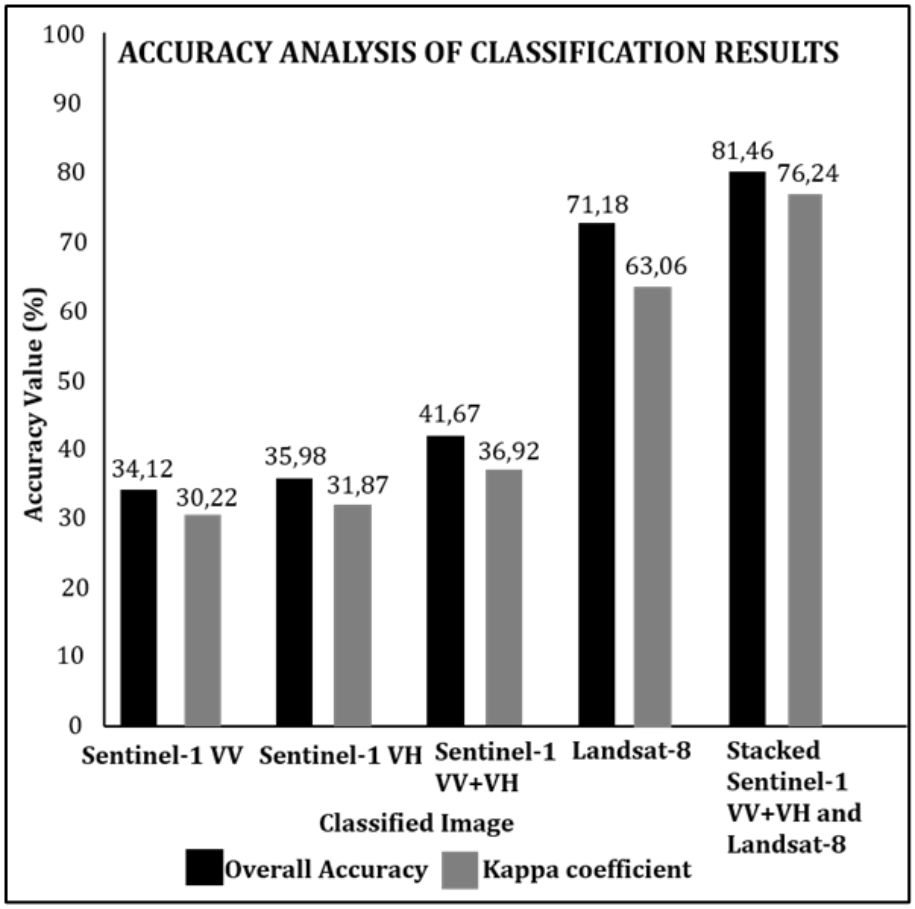

Figure 4. Overall accuracy and kappa coefficient values computed based on different data sets

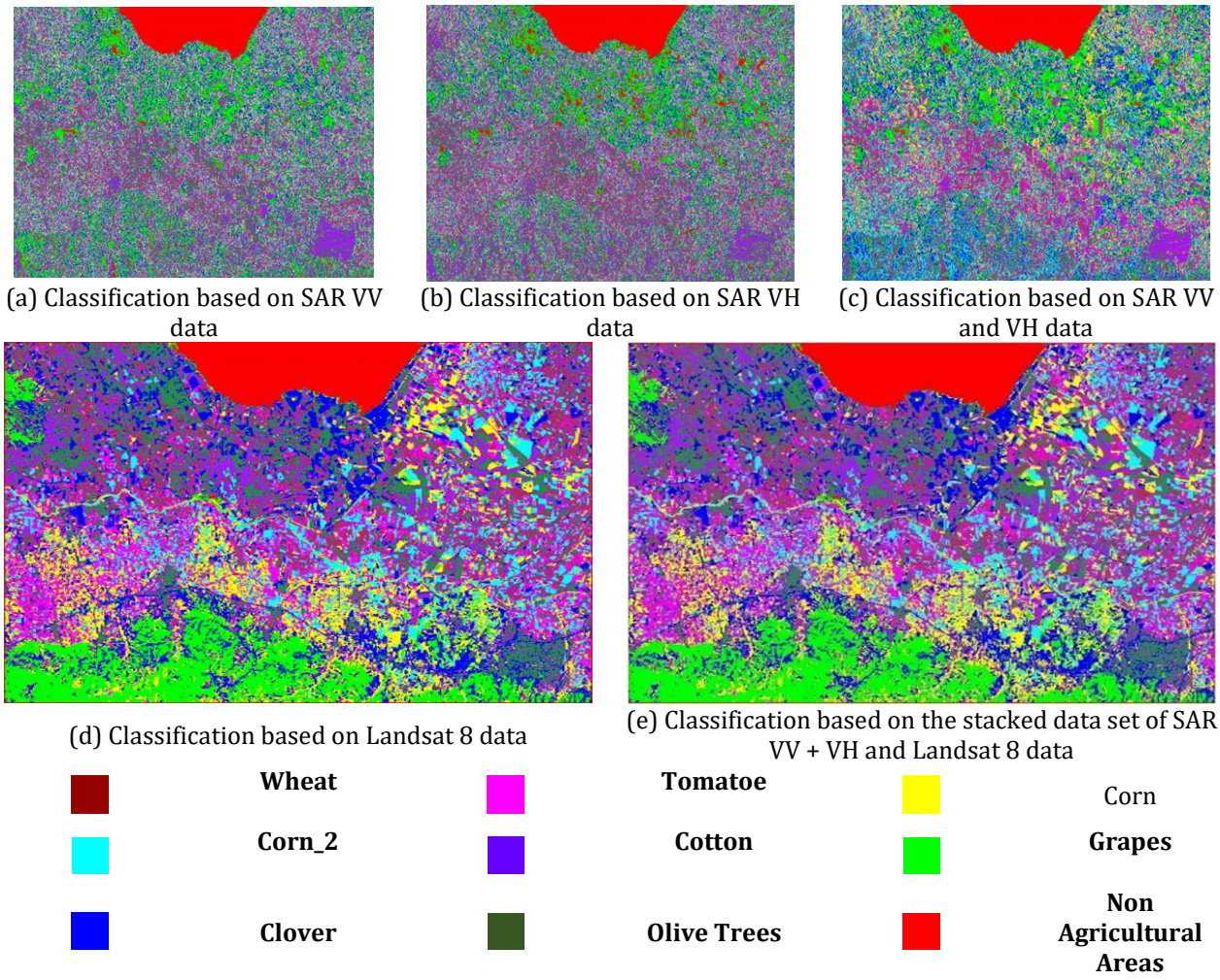

Figure 5. Comparison of the classifications conducted based on different data sets

The overall accuracy of the classification based on Sentinel-1 VV data was calculated as 34.12% and the Kappa coefficient value was calculated as 30.22%. For wheat, the PA and UA values were calculated as 48.00% and 48.42%, respectively. Similarly, these values respectively were 30.57% and 32.11% for tomato, 36.76% and 42.59% for corn, 22.71% and 25.64% for corn_2, 36.04% and 41.87% for cotton, 42.99% and 47.41% for grapes, 41.51% and 39.79% for clover, and 25.52% and 29.65% for olive trees. Corn_2 exhibited the lowest PA and UA values, while wheat provided the highest accuracy values.

The overall accuracy of the classification based on Sentinel-1 VH data was calculated as 35.98% and the Kappa coefficient value was computed as 31.87%. The PA and UA values for wheat were 50.62% and 51.06%, respectively. Similarly, these values respectively were 32.23% and 33.86% for tomatoes; 38.76% and 44.91% for corn; 23.94% and 27.03% for corn_2; 38.00% and 44.15% for cotton; 45.33% and 49.99% for grapes; 43.78% and 41.96% for clover; and 26.91% and 31.27% for olive trees. In the classification based on this data set, corn_2 exhibited the lowest PA and UA values, while wheat provided the highest accuracy values.

For the classification based on Sentinel-1 VV and VH bands separately, the values of PA, UA, overall accuracy, and Kappa coefficients generally stayed below 50%. This is due to the fact that the VV or VH band is a single-band panchromatic data that significantly affects the classification accuracy. It is evident that if only one of the Sentinel-1 VV or VH bands is used in the classification, the crops grown in this region cannot be reliably detected.

Comparing the overall accuracy values computed based on the Sentinel-1 VV and VH bands, the VH band provided approximately 1.86% better performance than the VV band. Similarly, the Kappa coefficient value computed for the VH band was slightly higher than the value computed for the VV band.

For the classification based on both Sentinel-1 VV and VH bands, the overall accuracy and Kappa coefficient values were calculated as 41.67% and 36.92%, respectively. For each crop type, the computed producer's and user's accuracy values were respectively as follows: 58.62% and 59.13% for wheat; 37.33% and 39.11% for tomato; 44.89% and 52.01% for corn; 27.73% and 31.31% for corn_2; 44.01% and 51.13% for cotton; 52.50% and 57.90% for grapes; 50.70% and 48.60% for clover; 31.17% and 36.21% for olive trees.

Classification based on the Sentinel-1 VV and VH bands together produced approximately 5% better results than using each of these bands alone. These findings confirm the generalization in this study that when there is an

increase in the number of bands included in the classification, there is a proportional increase in the classification results.

Classification based on Landsat-8 data only provided 71.18% overall accuracy and 63.06% Kappa coefficient value. The PA (60.10%) and UA (64.55%) values computed for wheat were lower than expected. For other crop types, the computed PA and UA values are respectively as follows: 76.16% and 78.33% for tomatoes; 66.28% and 72.73% for corn; 81.16% and 80.58% for corn_2; 80.72% and 77.14% for cotton; 74.19% and 74.87% for grapes; 76.12% and 77.76% for clover, and 71.63% and 73.90% for olive trees. Compared to Sentinel-1 SAR data (VV, VH and VV+VH), the Landsat-8 data provided up to 37% better performance in the overall accuracy. For Kappa coefficient, the accuracy increase was about 33% in favor of the Landsat-8 data. For the individual crop types, the UA and PA values were approximately 30% higher than that of Sentinel-1 SAR data. Although the spatial resolution of the Landsat-8 optical bands is 30 m and the spatial resolution of the Sentinel-1 VV and/or VH bands is 10 m, the classification accuracy based on Landsat-8 data was significantly higher than that of Sentinel-1 data. In this respect, we can say that the lower spatial resolution multi-band Landsat-8 optical data may be preferred to Sentinel-1 SAR data. In addition, our findings showed that the color effect of pixels or objects (agricultural parcels for this study) appears to be more important than the size (spatial resolution) factor that the pixels occupy on the ground.

Classification based on the stacked data set of Sentinel-1 VV + VH and Landsat-8 provided the overall accuracy and Kappa values of 81.46% and 76.24%, respectively. Based on the study of [37] we can say that these values are sufficient. This data set provided the highest overall accuracy and Kappa coefficient values of the datasets used. For the individual crop types, the computed PA and UA values were, respectively as follows: 62.98% and 68.86% for wheat; 73.06% and 82.08% for tomatoes; 78.13% and 75.54% for corn; 89.79% and 88.58% for corn_2; 81.91% and 80.34% for cotton; 89.27% and 88.31% for grapes; 88.60% and 87.10% for clover and 86.65% and 91.46% for olive trees. It is evident that the use of the stacked data set of Sentinel-1 VV+ VH and Landsat 8 in the classification significantly improved the results when compared the use of either of these images. The use of the stacked Sentinel-1 VV+VH and Landsat 8 data set in the classification provided much better performance than that of using either of these images (Table 3 and Figure 4).

For the classification based on Sentinel-1 VV, VH, and VV+VH, wheat provided the highest PA and UA accuracy values (Table 3). On the other hand, for the classification based on Landsat-8 and the stacked data set of Sentinel-1 VV+VH and Landsat-8, wheat gave the lowest PA and UA accuracy values. This is due to the presence of interpretation elements of SAR and optical images that may be inferior or superior to each other. The characteristics of SAR images are different from optical ones. Optical image classification is highly correlated with texture and shape information, while SAR image classification relies more on shape information because the texture is always blurred and full of noise [35]. In this study, the existence of this situation has been monitored only for the wheat crop type.

5. Conclusion and Recommendation

This study investigated the effect of the integration of single date (07.06.2017) Sentinel-1 SAR and Landsat-8 data on the classification performance of agricultural summer crops. The integration of these two data sets was carried out at feature level through image stacking and supervised RF machine learning algorithm was used for classification. Image classification was performed using different image data sets. Classification conducted using the original Sentinel-1 VV or VH polarized bands provided accuracy values about 35%. The use of both Sentinel-1 VV and VH bands in classification exhibited a marginal effect in the results increasing overall accuracy to 41.67%. The results show that a single-date Sentinel-1 SAR VV or VH data is not sufficient in detecting summer crops, at least in the area used in this study. Classification based on Landsat-8 data only provided much higher overall accuracy (71.18%) than that of Sentinel-1 data. According to [36], this accuracy value is reasonable. This higher accuracy value demonstrates that multispectral-bands have considerable contribution to classification of a single-date image.

Classification based on the stack dataset of the integrated Sentinel-1 VV + VH and Landsat-8 provided overall accuracy and Kappa values of 81.46% and 76.24%, respectively. Among the input image datasets used in this study, this data set provided the best results. When used alone, the Sentinel-1 SAR data (VV or VH band) provided considerably low accuracy values. However, when combined with Landsat 8 optical image, Sentinel-1 SAR data demonstrated a significant contribution to results.

The FRS data are prepared based on the verbal statements of the farmers. In order to use FRS data as reference data for training and accuracy assessment, it should undergo some editing operations. Those FRS parcels with missing or incorrect information such as cultivated area, cultivated crop name, difference between total parcel area and cultivated area, etc. can be automatically detected and corrected in the database.

The use of both Sentinel-1 SAR and Landsat-8 optical images in classification provides the combined effects of higher spatial resolution SAR bands and lower spatial resolution multispectral bands. Classification based on the stack dataset of the integrated image of these two data sets appears to provide sufficient accuracy values for agricultural crop type detection in regions with reasonably large agricultural fields. The study has shown that the

stacked dataset of Sentinel-1 VV+VH and Landsat-8 belonging to a single date has great potential in extracting summer crop types.

Acknowledgement

The authors would like to thank Turkish Republic of Ministry and Forestry for providing the FRS reference data.

Funding

This research received no external funding.

Author contributions

Muslum Altun: Conceptualization, Methodology, Software, Data curation, Writing-Original draft preparation, Validation. **Mustafa Turker:** Conceptualization, Visualization, Investigation, Writing-Reviewing and Editing.

Conflicts of interest

The authors declare no conflicts of interest.

References

1. Gumma, M. K., Nelson, A., Thenkabail, P. S., & Singh, A. N. (2011). Mapping rice areas of South Asia using MODIS multitemporal data. Journal of Applied Remote Sensing, 5(1), 1-26.
2. Thenkabail, P. S., Hanjra, M. A., Dheeravath, V., & Gumma, M. (2011). Global croplands and their water use remote sensing and non-remote sensing perspectives. Weng Q (Ed.), Advances in Environmental Remote Sensing: Sensors, Algorithms, and Applications, (pp. 383-419). Florida, CRC Press.
3. Viskovic, L., Kosovic, I. N., & Mastelic, T. (2019, September). Crop classification using multi-spectral and multitemporal satellite imagery with machine learning. In 2019 International Conference on Software, Telecommunications and Computer Networks (SoftCOM) (pp. 1-5). IEEE.
4. Altun, M. & Türker, M. (2021). Çoklu zamanlı Sentinel-2 görüntülerinden tarımsal ürün tespiti: Mardin – Kızıltepe örneği. Afyon Kocatepe Üniversitesi Fen Ve Mühendislik Bilimleri Dergisi, 21 (4), 881-899.
5. Lemoine, G., & Leo, O. (2015, November). Crop mapping applications at scale: Using google earth engine to enable global crop area and status monitoring using free and open data sources. In International Geoscience and Remote Sensing Symposium, (IGARSS) (pp. 1496-1499). IEEE.
6. Lussem, U., Hütt, C., & Waldhoff, G. (2016, July). Combined analysis of Sentinel-1 and Rapid Eye data for improved crop type classification: An early season approach for rapeseed and cereals. International Archives of the Photogrammetry, Remote Sensing and Spatial Information Sciences, 41(2016), 959-963.
7. Foody, G. M., M. B. Mcculloch, M. B., & W. B. Yates, W.B. (1994). Crop classification from C-band polarimetric radar data. International Journal of Remote Sensing, 15(14), 2871-2885.
8. Skriver, H. (2012). Crop classification by multitemporal C- and L-band single- and dual polarization and fully polarimetric SAR. IEEE Transactions on Geoscience and Remote Sensing, 50(6), 2138-2149.
9. Sonobe, R., Tani, H., Wang, X., Kobayashi, N., & Shimamura, H. (2014). Random forest classification of crop type using multi-temporal TerraSAR-X dual-polarimetric data. Remote Sensing Letters, 5(2), 157-164.
10. Siachalou, S., Mallinis, G., & Tsakiri-Strati, M. (2015). A hidden markov models approach for crop classification: Linking crop phenology to time series of multisensor remote sensing data. Remote Sensing, 7(4), 3633-3650.
11. Altun, M. & Türker, M. (2022). Kaynaştırılmış Sentinel-1 SAR ve Landsat-8 optik veriden makine öğrenme algoritması ile tarımsal ürün tespiti . Turkish Journal of Remote Sensing and GIS, 3 (1) , 1-19.
12. Chen, S., Useya, J., & Hillary Mugiyo, H. (2020). Decision-level fusion of Sentinel-1 SAR and Landsat 8 OLI texture features for crop discrimination and classification: case of Masvingo, Zimbabwe. Heliyon, 6(11), 1-14.
13. Nuthammachot, N., & Stratoulias, D. (2019). Fusion of Sentinel-1A and Landsat-8 images for improving land use/land cover classification in Songkla Province, Thailand. Applied Ecology and Environmental Research, 17(2), 3123-3135.
14. Otukei, J. R., Blaschke, T., & Collins, M. (2015). Fusion of TerraSAR-x and Landsat ETM+ data for protected area mapping in Uganda. International Journal of Applied Earth Observation and Geoinformation, 38, 99-104.
15. Suwarsono, N., Prasasti, I., Nugroho, J. T., Sitorus, J., & Triyono, D. (2018). Detectıng the lava flow deposıts from 2018 anak krakatau eruptıon usıng data fusıon Landsat-8 optıc and Sentınel-1 SAR. International Journal of Remote Sensing and Earth Sciences, 15(2), 157-166.

16. Dimov, D., Kuhn, J., & Conrad, C. (2016, July). Assessment of cropping system diversity in the fergana valley through image fusion of Landsat 8 and Sentinel-1. In 23rd ISPRS Congress, 2016. (pp.173-180). XXIII ISPRS.
17. Cao, J., Cai, X., Tan, J., Cui, Y., Xie, H., Liu, F., Yang, L., & Luo, Y. (2020). Mapping paddy rice using Landsat time series data in the Ganfu Plain irrigation system, Southern China, from 1988-2017. International Journal of Remote Sensing, 42(4), 1556-1576.
18. Forget, Y., Shimoni, M., Gilbert, M., & Linard, C. (2018). Complementarity Between Sentinel-1 and Landsat 8 Imagery for Built-Up Mapping in Sub-Saharan Africa. 10.20944/preprints201810.0695.v1.
19. Zhang, H., & Xu, R. (2018). Exploring the optimal integration levels between SAR and optical data for better urban land cover mapping in the Pearl River Delta. International Journal of Applied Earth Observation and Geoinformation, 64(2018), 87-95.
20. Copernicus. (2021, Mart 30). Copernicus Open Access Hub. https://scihub.copernicus.eu/dhus/#/home
21. EarthExplorer. (2021, Mart 30). USGS Earth Explorer. https://earthexplorer.usgs.gov
22. T.C. Tarım ve Orman Bakanlığı. (2021, Mart 30). T.C. Tarım ve Orman Bakanlığı. https://www.tarimorman.gov.tr/
23. ESA Copernicus Open Access Hub. (2021, Mart 30). Overview, Sentinel-1 Data Offer. https://scihub.copernicus.eu/userguide/
24. Lee, J.S., Jurkevich, I., Dewaele, P., Wambacq, P., & Oosterlinck, A. (1994). Speckle filtering of synthetic aperture radar images: A review. Remote Sensing Reviews, 8(4), 313-340.
25. Filipponi, F. (2019). Sentinel-1 GRD preprocessing workflow. Multidisciplinary Digital Publishing Institute Proceedings, 18(1), 11-15.
26. ArcGIS User Guide. (2021, Nisan 22). ArcGIS Desktop User Guide Documentation, https://desktop.arcgis.com/en/documentation/
27. Erdas Imagine User Guide. (2021, Nisan 22). Hexagon Erdas imagine user guide. https://www.hexagongeospatial.com/
28. Witharana, C., Civco, D. L., & Meyer, T. H. (2013). Evaluation of pansharpening algorithms in support of earth observation based rapid-mapping workflows. Applied Geography, 37(2013), 63-87.
29. MathWorks. (2021, Mayıs 8). MathWorks Makers of MATLAB and Simulink. https://www.mathworks.com/
30. Liaw, A., & Wiener, M. (2002). Classification and regression by random forest. R News, 2(3), 18-22.
31. Pal, M. (2005). Random forest classifier for remote sensing classification. International Journal of Remote Sensing, 26(1), 217-222.
32. Utgoff, P. E., & Brodley, C. E. (1990). An incremental method for finding multivariate splits for decision trees. In Machine Learning Proceedings 1990, (pp. 58-65), Morgan Kaufmann.
33. Pal, M., & Mather, P. M. (2003). An assessment of the effectiveness of decision tree methods for land cover classification. Remote Sensing of Environment, 86(4), 554-565.
34. Campbell, J.B., & Wynne, R.H. (1996). Introduction to remote sensing. New York, London, Guilford Press.
35. Guo, Y., Pan, Z., Wang, M., Wang, J., & Yang, W. (2020). Learning Capsules for SAR Target Recognition. IEEE Journal of Selected Topics in Applied Earth Observations and Remote Sensing, 13(1), 4663-4673.
36. Cohen, J. (1960). A coefficient of agreement for nominal scales. Educational and Psychological Measurement, 20(1), 37-46.